RevMexAA (Serie de Conferencias), **2**, 105-113 (1995)

GAS AND DUST IN THE CARINA NEBULA[1]

P. Cox

Observatoire de Marseille, 2 pl. Leverrier, F-13248 Marseille Cedex 4, France

Max-Planck-Institut für Radioastronomie, Postfach 2024, D-53121 Bonn, Germany

RESUMEN

Se presenta una revisión de la morfología del gas y el polvo en la nebulosa de Carina basada en nuevas observaciones milimétricas de emisión en CO y mapas en infrarrojo y radio. Se describen las propiedades físicas del gas neutro, tales como calentamiento y enfriamiento, la penetración de la radiación ultravioleta en las nubes moleculares, la influencia de los vientos estelares sobre el gas molecular, y la estabilidad y dinámica de las condensaciones detectadas en CO.

ABSTRACT

This review describes the large scale structure of the gas and dust in the Carina Nebula based on new high-resolution maps of millimeter CO emission together with infrared and radio measurements. The physical conditions of the neutral gas are described including heating and cooling, the penetration of the ultraviolet radiation inside the molecular clouds, the influence of the stellar winds on the molecular gas, and the stability and dynamics of the clumps identified from the CO studies.

Key words: **DUST, EXTINCTION — ISM: INDIVIDUAL OBJECTS (CARINA NEBULA) — ISM: MOLECULES — STARS: FORMATION**

1. INTRODUCTION

The Carina Nebula is certainly the nearest-by example of a region of very massive star formation. The open cluster Trumpler 16 (Tr 16) is centered on the peculiar star Eta Carinae (η Car), which is one of the most luminous galactic sources and is regarded as an extreme case of a Luminous Blue Variable. The tighter group of stars designated Tr 14 lies 10 arcmin to the north of η Car. Both clusters are exceptionally rich in highly luminous and massive stars, including six of the eleven known O3 spectral type stars of the Galaxy in addition to η Car and a Wolf-Rayet star, both massive evolved objects (Walborn 1995). Such a high concentration of the earliest-type stars remains unique outside of 30 Doradus in the Large Magellanic Clouds —see e.g., Walborn (1991). As compared to 30 Doradus, the Carina Nebula , which at a distance of 2.5 kpc (Feinstein 1995), is about 15 times nearer than the LMC, offers the opportunity to study in detail the interaction of the most massive stars known with their immediate surroundings. This interaction, which is largely dominated by the ionizing flux and the stellar winds from the massive stars, shapes the region as we can see it today.

In this paper, we review earlier observations of the neutral gas in the Carina Nebula and summarize the results of a new survey of millimeter CO emission together with recent infrared and radio studies.

[1]Based on observations collected at the European Southern Observatory, La Silla, Chile.

2. PREVIOUS STUDIES

It was in 1838, during the brightening of η Car, that J. Herschel made his famous drawing of the Carina Nebula recording with remarkable precision the details of the gaseous nebula and the many interwoven obscuration patches and dust lanes. This is the first record of the gas and dust content of the Carina Nebula showing the well-known morphology of its brightest part along the region extending from Tr 16 to Tr 14. Modern photographs such as published by Walborn (1975) and Malin (1993) further reveal the details of the two prominent dust lanes forming a V-shaped structure which enclose the two clusters of luminous, massive stars and are bordered by numerous bright rims and cometary globules.

The influence of the exceptional stellar content of the Carina Nebula, already seen in the intricate optical morphology, was further revealed by the complex velocity structure measured in the ionized gas both in optical (Deharveng & Maucherat 1975) and radio (Huchtmeier & Day 1984) line emission and in the associated neutral gas (Walborn, Blanco, & Tackeray 1984). It was shown that these kinematics (expanding large-scale structures) are linked with the stellar winds ejected by the most massive members of the clusters.

Molecular absorption measurements in H_2CO (Gardner, Dicke, & Whiteoak 1973) and OH (Dickel & Wall 1974) indicated that the neutral gas was mostly concentrated along the dark bays which was later confirmed by the maps made in the 230 GHz ^{12}CO(2-1) line by de Graauw et al. (1981). Although measured with a large beam (2′2) and a crude sampling (4′4), these maps showed that the overall distribution of the CO emission follows the V-shaped dust lane and indicated additional molecular gas north of Tr 14. Whiteoak & Otrupcek (1984) carried out a survey of the northern part of the Carina Nebula in the 115 GHz ^{12}CO(1-0) line using a 2′8 beam and a sampling of 3 arcmin which further illustrated how closely the molecular gas follows the dark lanes and traced in more detail the distribution of the molecular gas in the north. The complete ^{12}CO(1-0) survey by Grabelsky et al. (1988) done at Cerro Tololo with the 1.2-meter telescope (8′8 beam) demonstrated that the Carina Nebula is part of a giant molecular cloud complex extending over about 130 pc with a mass in excess of $5 \times 10^5\ M_\odot$. This giant molecular cloud is very likely to be the parent material of the OB associations Tr 14 and Tr 16.

The clouds shaping the dark lanes were also mapped at far-infrared wavelengths by Harvey, Hoffman, & Campbell (1978) at 80 μm and subsequently by Gosh et al. (1988) who observed the entire nebula at 120–300 μm. Both studies showed that the infrared emission correlates with the dark clouds and that the dust in the surrounding molecular clouds absorbs and re-radiates in the infrared the intense ultraviolet and visible radiation from the nearby massive stars.

The picture emerging from these studies is one of a concentration of very massive stars interacting with the parental giant molecular cloud, ionizing the diffuse gas, heating and photodissociating the molecular gas, and inducing dynamical disruption of the clouds through stellar winds.

We have undertaken extensive survey work using the SEST 15-meter telescope in order to study both at high spatial (25 arcsec corresponding to a linear scale of 0.3 pc for the adopted distance of 2.5 kpc to the Carina Nebula) and spectral resolution ($\sim$ 0.2 km s^{-1}) the molecular gas content of the Carina Nebula. Most of the molecular gas associated with Tr 14 and Tr 16 has been mapped. This work has been complemented by high spatial resolution *IRAS* maps. We also present high-resolution and sensitivity radio maps recently obtained by Whiteoak (1994) (Figure 1). We summarize the main results of this work in progress and comment on some of the issues raised by the observations.

3. RECENT OBSERVATIONS

3.1. Radio Observations

Previous radio surveys of the Carina Nebula (Gardner et al. 1970; Retallack 1983; Tateyama, Strauss, & Kaufmann 1991) showed the presence of two main peaks of emission associated with Tr 14 and Tr 16 hereafter Car I and Car II, respectively. Recently, Whiteoak (1994) published a radio continuum survey of the entire Carina Nebula done at 0.843 GHz using the Molonglo Observatory Synthesis Telescope with a spatial resolution of 43 × 53 arcsec^2. These observations revealed the details of the morphology of Car I and Car II and additional, weaker emission in between them. Figure 1 displays the 0.843 GHz image of the Car I/Car II complex. To the north-west, in the vicinity of Tr 14 a radio plateau is seen which extends along the boundary of the prominent dark dust lane and the optical nebulosity. This morphology is clearly suggesting an ionization front bordering a dense dust/molecular cloud. To the south, the radio contours exactly follow the filaments seen in the optical photographs around η Car —see also Retallack (1983). South of these filaments a sharp gradient in the radio emission is present indicating that the regions south of η Car may be devoid of gas. Many fainter, filamentary

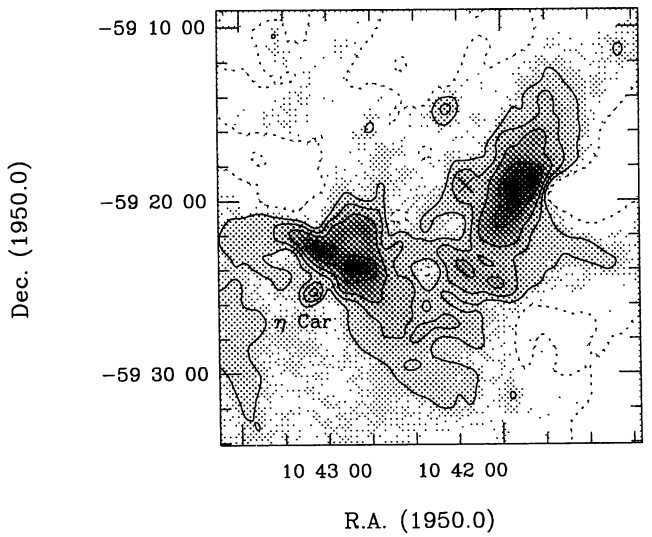

Fig. 1. The distribution of the ionized gas in the Carina Nebula around the stellar clusters Tr 14 (shown by a cross) and Tr 16 (the position of η Car is indicated). The radio image at 0.843 GHz has a resolution of 43″ × 53″ (from Whiteoak 1994). Contours are drawn at 0.2 (dashed), 0.4, 0.5, 0.9, 1.4, 1.7, and 1.9 Jy beam^{-1}.

radio structures are also present in between the Car I and Car II complexes. An important result of the 0.843 GHz survey is the lack of nonthermal radio emission. This fact may imply an absence of supernovae remnants and indicate that the stellar clusters in the Carina Nebula are young, i.e., $\sim 10^6$ yr in agreement with other studies (Feinstein 1995; Walborn 1995).

3.2. The *IRAS* Maps

High-resolution images of the Carina Nebula around Tr 14 and Tr 16 are presented in Figure 2 in the four *IRAS* bands at 12, 25, 60, and 100 μm. The resolutions of the *IRAS* maps are 40″ at 12 and 25 μm, 1′.0 at 60 μm and 1′7 at 100 μm, respectively. They have been obtained by P.J. Roelfsema who used the HIRAS system developed at the Department of Space Research (Groningen, The Netherlands) which is a routine based on a maximum entropy reconstruction of the *IRAS* survey data. For a description of the HIRAS system we refer to Bontekoe, Koper, & Kester (1994).

The *IRAS* maps show three main emission regions most clearly defined in the 100 μm map. i) The region around η Car displaying emission which extends along an east-west direction and is associated with the filaments traced in the radio continuum maps. This region of warm dust dominates the infrared maps at 12 and 25 μm. ii) The northern region around Tr 14 which is the brightest region of the Carina Nebula at 60 and 100 μm. This is the region which was first mapped by Harvey et al. (1978). At 12 and 25 μm, the infrared emission peaks on the cluster Tr 14 and shows to the west an elongated plateau of emission corresponding to the radio plateau. At longer wavelengths, the distribution of the infrared emission shifts farther to the west, away from the heating sources and aligned with the obscuration lane. iii) The third region delineated in the *IRAS* maps corresponds to the dark lane extending south of η Car. The east-west extension of the infrared contours precisely follow the shape of the ionization fronts beautifully seen in the optical picture published by Walborn (1975). A 8-shaped dust cloud (best seen at 60 μm but also at 12 μm) dominates this region together with a small cloud associated with the source IRAS 10430–5931 (Figure 3). This 8-shaped cloud was also detected in the 120–300 μm maps published by Ghosh et al. (1988). As is the case for the radio continuum emission, the region in between η Car and the southern dark bay, which contains the numerous luminous and massive stars of the open cluster Tr 16, is also a region of weak infrared emission.

The infrared morphology changes significantly from one *IRAS* band to the other. Whereas the 25 μm emission is almost similar to the radio continuum emission (Fig. 1), the emission seen at 60 and 100 μm is shifted towards the warm, dense parts of the molecular clouds (see below). The 12 μm emission (tracing the distribution of transiently heated small dust particles) peaks in between the distributions of the 25 and

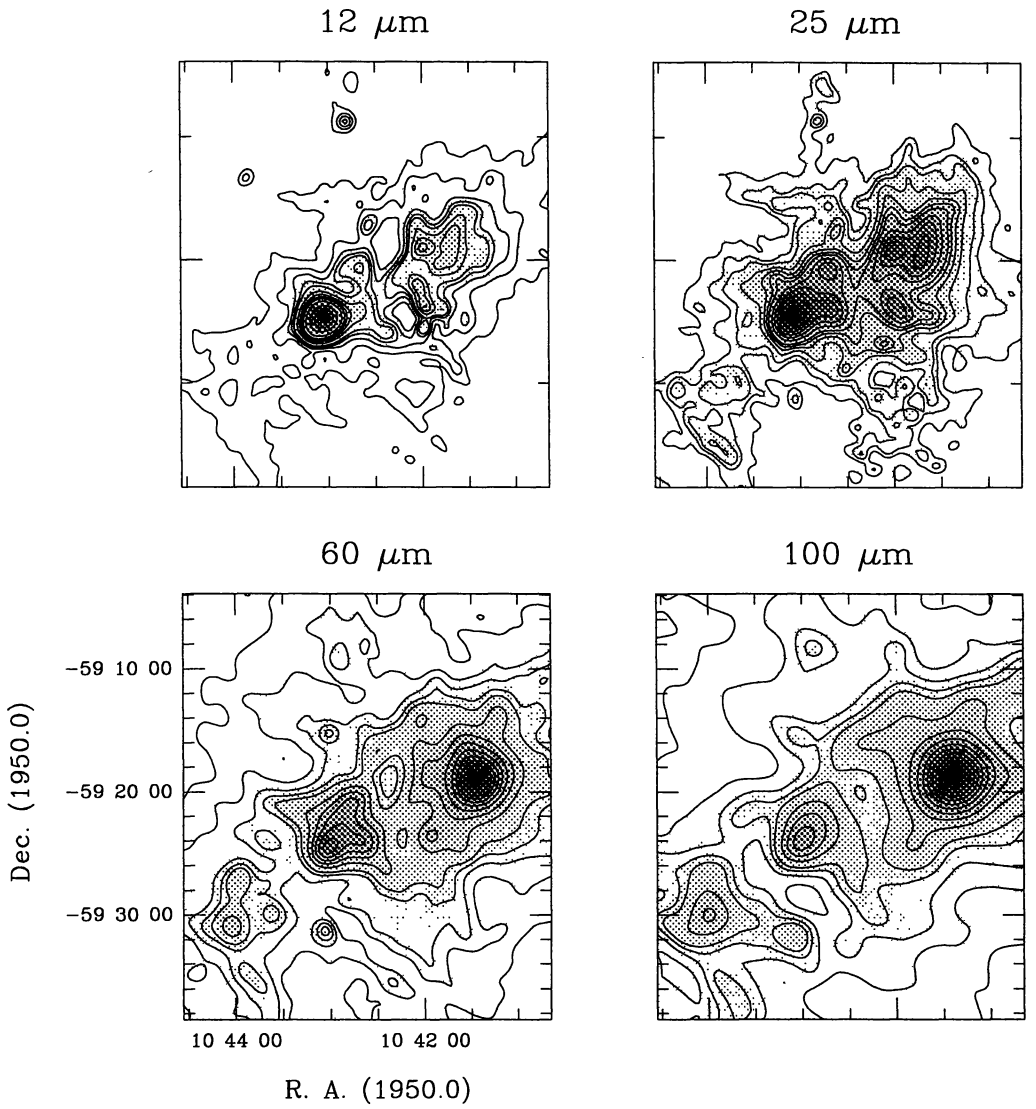

Fig. 2. High-spatial resolution *IRAS* images of the Carina Nebula at 12, 25, 60 and 100 μm (a to d). The contours, in units of MJy sr^{-1}, are as follows: 100 to 500 by step of 100 (100:500:100), 750:1500:250, 2000:5000:1000, 7500:15000:2500 at 12 μm; 500:1000:250, 1500, 2000, 2500, 3000:10000:1000 at 25 μm; 1000:5000:1000, 7500:30000:2500 at 60 and 100 μm. In the present maps, no corrections were applied for the saturation effects induced by the extremely high infrared flux densities of η Car.

60/100 μm emissions. The clear tendency for the infrared distribution to peak at the position of the molecular emission as one goes from the mid to the far-infrared implies the presence of a strong temperature gradient likely caused by the external heating from the O stars associated with Tr 16 for the southern cloud and Tr 14 for the northern cloud.

Most of the point sources are detected at 12 μm and are associated with stars. In contrast, there appears to be few embedded *IRAS* sources with the exception of IRAS 10430–5931. An overall diffuse envelope of infrared emission is seen in all the *IRAS* bands pointing away from the core of the Carina Nebula in the form of extended, curved filaments. This emission accounts for a significant fraction of the infrared luminosity of the Carina complex and could be related to the escape of the ultraviolet photons emitted by the numerous massive stars present in the nebula —see also Ghosh et al. (1988).

3.3. The Molecular Gas Distribution

The CO line emission of the molecular clouds facing the stellar clusters Tr 14 and Tr 16 are displayed as velocity integrated contours in ^{13}CO(1–0) and ^{12}CO(2–1), respectively, on the underlying gray scale image and contours of the *IRAS* 60 μm emission. The similarities in the distribution of the dust and CO line emission is remarkable. South of η Car, the CO contours follow the infrared contours along the east-west extension

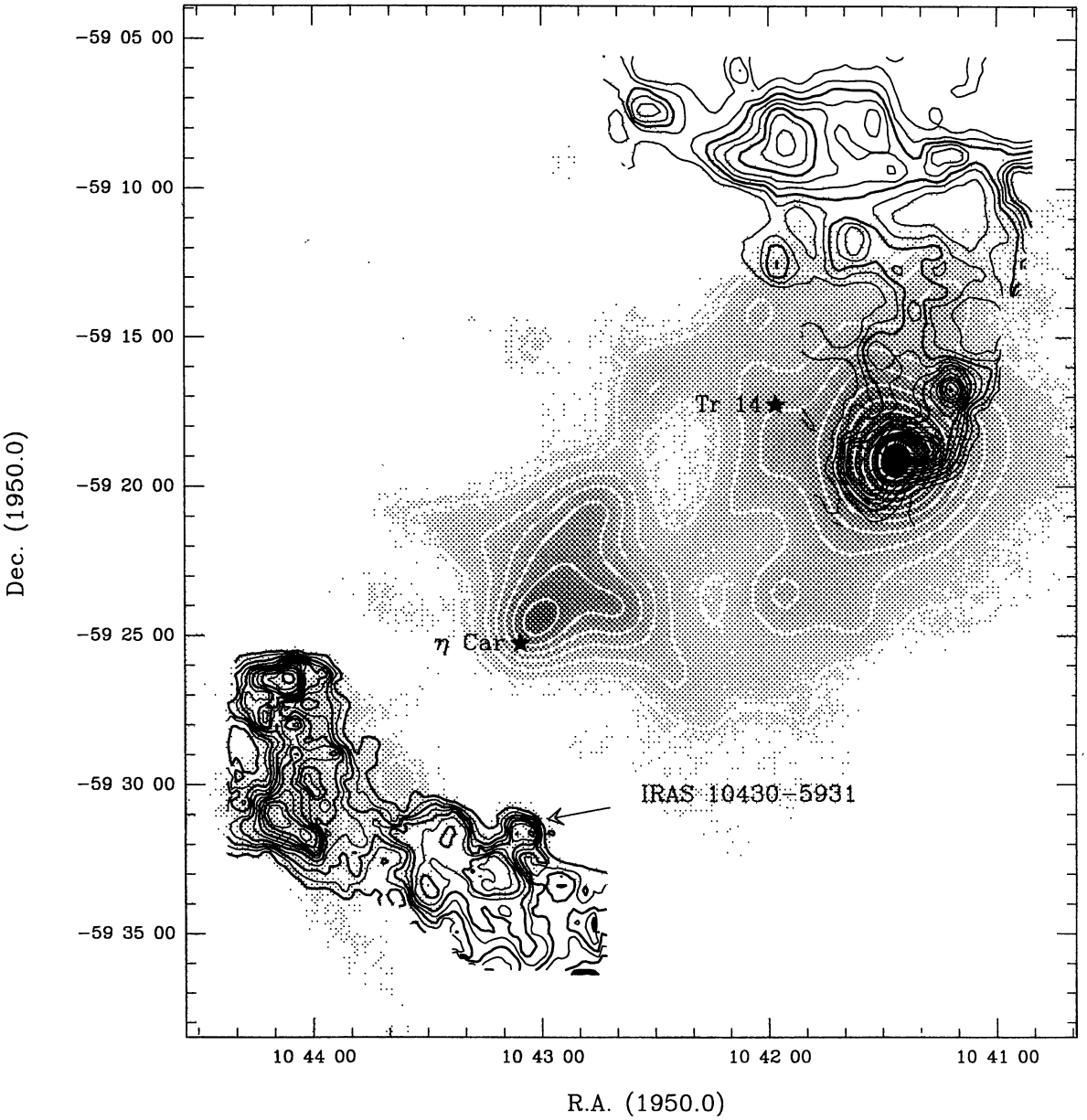

Fig. 3. Composite figure showing the *IRAS* 60 μm emission (gray scale and white contours as in Figure 2) and the distribution of the CO emission in the Carina Nebula (black contours). The northern molecular cloud around Tr 14 has been mapped in ^{13}CO(1–0) with a beam of 50″ and the southern cloud associated with Tr 16 in ^{12}CO(2–1) with a beam of 25″. The positions of η Car, Tr 14 and the embedded source IRAS 10430–5931 are indicated. The ^{13}CO(1–0) contours (showing the emission integrated over the velocity range −17 to −23 km s^{-1}) go from 4 to 32 by 2; the ^{12}CO(2–1) contours (showing the emission in the range −28 to −22 km s^{-1}) are shown from 10 to 80 by 7 (in units of K km s^{-1}).

of the dark lane. The 8-shaped infrared cloud reflects the morphology of the CO cloud although the infrared distribution is shifted westwards, i.e., towards the heating sources of Tr 16. The fact that this morphology is also traced at 12 μm (Fig. 2) indicates unusual warm molecular gas. The velocity field of this southern cloud is also very peculiar. Double ^{12}CO, ^{13}CO, and C^{18}O profiles are measured in its center implying a high velocity dispersion (the velocity difference is of the order of 8 km s^{-1}). As shown in Cox, Bronfman, & Roelfsema (1995), the most likely explanation for this velocity dispersion is that the whole cloud is torn apart by the impinging stellar winds from the most massive members belonging to Tr 16.

Further influence of the stars belonging to Tr 16 may be seen in the presence of the *IRAS* source (IRAS 10430–5931) which is located in a small CO cloud defining a clear cone-shaped structure at the interface between the molecular/dust cloud and the ionized gas (Figure 4). Near-infrared images results in the J, H, and K'-bands done at Las Campanas (Megeath et al. 1994) of the surroundings of this embedded source have revealed a number of reddened sources dominated by one strong, highly reddened source possibly of spectral type B0 (see Fig. 4). The distinct patch of nebulosity seen at the edge of the globule is probably due to reflection. This is the first evidence for on-going star formation in the Carina Nebula and appears to be a strong case of implosive star formation. Such triggered star formation, which has been investigated theoretically by Bertoldi (1989), occurs when molecular clumps lying at the periphery of the H II region and the main molecular cloud are suddenly exposed to the ionized radiation from nearby, newly formed massive stars.

The molecular gas facing Tr 14 consists of two main clouds. The brightest one which corresponds to the far-infrared emission peak has a mass of about $10^5\,M_\odot$. It shows two ^{13}CO clouds which are precisely aligned with the dark dust lane. As compared to the molecular gas associated with Tr 16, the morphology of the molecular cloud facing Tr 14 appears much tighter. Velocity channel maps of this molecular cloud reveal numerous molecular clumps characterized by a high velocity dispersion. As in the case of the molecular cloud facing Tr 16, the most likely explanation is that the stellar winds from Tr 14 impact on the surface of the northern cloud influencing both its structure and dynamics. But the more compact appearance of the cloud related to Tr 14 suggests that the interaction may have started somewhat later than in the case of Tr 16. A complete physical and chemical study of this outstanding photodissociation region will be presented in Cox, Bronfman, & Roelfsema (1995). Finally, the cloud north of Tr 14 is neither detected in the *IRAS* maps nor in the far-infrared maps published by Ghosh et al. (1988). It appears to be unaffected by the radiative field from Tr 14.

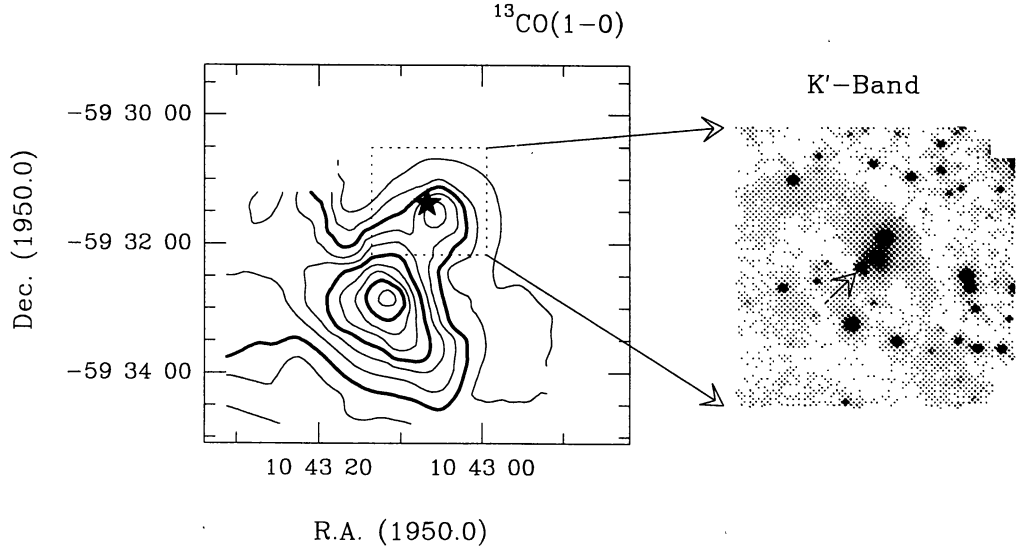

Fig. 4. a) ^{13}CO(1–0) map of the molecular gas in the vicinity of IRAS 10430–5931. The contours are from 2 to 29 by 3 K km s^{-1} and show the velocity integrated emission in the range −22 to −30 km s^{-1}. b) K'-Band image of the surroundings of IRAS 10430–5931 covering the area shown as a box in a). The arrow identifies the candidate B0 spectral type star (from Megeath et al. 1994).

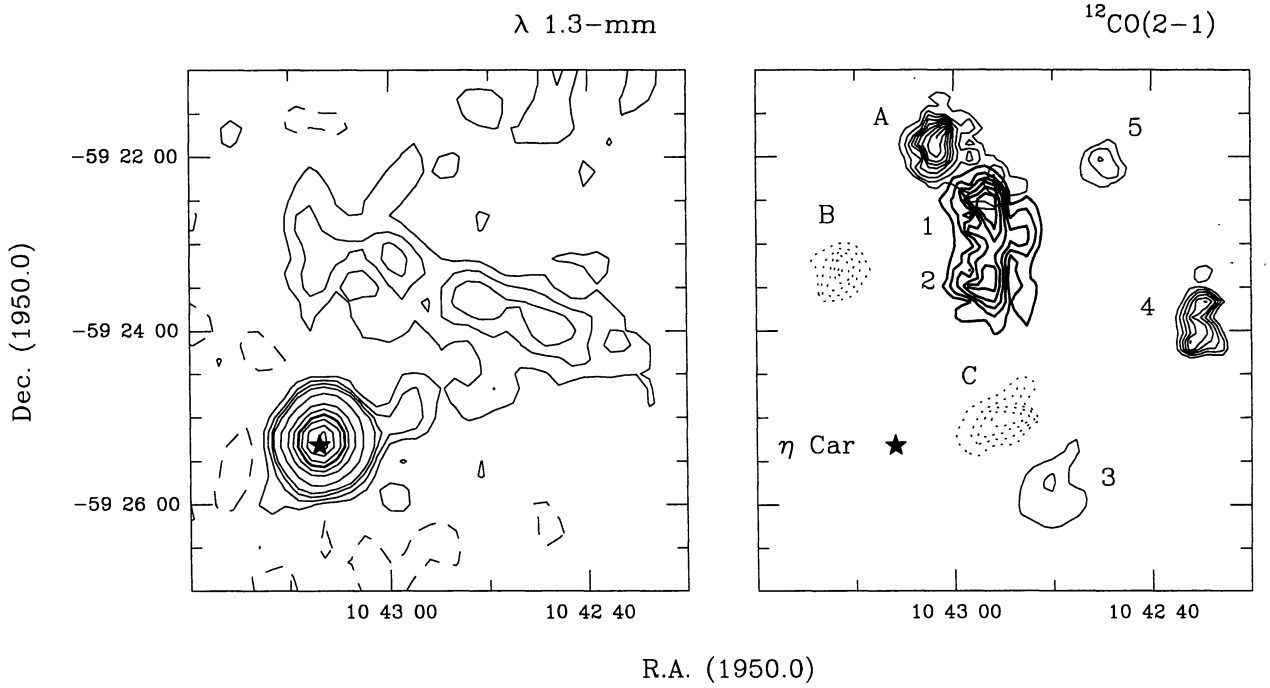

Fig. 5. Maps of the surroundings of η Car in the millimeter continuum (λ 1.3-mm) and ^{12}CO(2–1) line emission. The continuum image was obtained in August 1991 with an angular resolution of 30″ (adapted from Cox et al. 1995). Contours are -250 (dashed line), 250 to 1000 by 250, 2000 to 10000 by 2000, 130000, and 16000 mJy/beam. The peak value is 16 Jy/beam and is centered on η Car. The ^{12}CO(2–1) velocity integrated map shows the molecular clouds shaping the Keyhole nebula (from Cox & Bronfman 1995). The blue-shifted molecular gas is integrated from -34 to -31 km s^{-1} (Clouds 1 and 2) and from -31 to -22 km s^{-1} (Clouds 3, 4 and 5). The red-shifted gas contains Cloud A (-22 to -13 km s^{-1}) and Clouds B and C (-13 to -7 km s^{-1}). Contours are: 3 to 13 by 2 K km s^{-1}, except for Cloud A where contours are from 10 to 50 by 5 K km s^{-1}.

3.4. The Keyhole Nebula

The distribution and kinematics of the molecular gas associated with the Keyhole Nebula —the dense dark patch seen north-west of η Car (see Walborn 1975)— are displayed in Figure 5 where the ^{12}CO(2–1) integrated velocity contours are compared to the λ 1.3-mm continuum emission. The molecular gas is clearly clumpy with small (sizes of a few tenths of a parsec), distinct clouds whose velocities are spread by as much as 10 km s^{-1} around the systemic velocity of the Carina Nebula (-22 km s^{-1}). The λ 1.3-mm continuum map is dominated by the emission of η Car. Extended emission is also detected along the radio filaments tracing the optically thin free-free emission from the gas ionized by the nearby massive luminous stars of Tr 16. The anticoincidence between the millimeter continuum and line emission is remarkable and demonstrates that the gas in between the molecular clumps associated with the Keyhole Nebula is ionized.

The molecular clouds which are detected around η Car are characterized by masses of about 10 $M_\odot$ which are two orders of magnitude lower than the corresponding virial masses; an isothermal cloud with a velocity dispersion of $\sim$ 3 km s^{-1} and a size of $\sim$ 0.5 pc, characteristic of the clouds identified here, has a virial mass of about 900 $M_\odot$. The large discrepancy may be due to the fact that the clouds are supported by the external pressure from warm and diffuse gas which is ionized by the strong UV radiation field pertaining in this region. Assuming virial equilibrium, the pressure needed to bind the molecular clouds in the Keyhole Nebula is $P_{ext}/k = 8 \times 10^4$ K cm^{-3}. Such a pressure could easily be provided by the warm, low density ionized gas traced in the radio (Whiteoak 1994) and millimeter continua where the typical electron density is $\sim$ 100 cm^{-3} and the temperature amounts to a few 1000 K.

The kinematics of the molecular gas in the Keyhole Nebula (Figure 5) are comparable to those measured in

optical (Deharveng & Maucherat 1975) and radio recombination lines (Huchtmeier & Day 1975). Both delineate the surface of a large cavity expanding with a velocity of about 20 km s^{-1} which is powered by the kinetic energy mostly injected by η Car. The fact that the neutral globules flow together with the low-density ionized gas confirms that the dust clouds which give its appearance to the Keyhole Nebula are part of the whole Carina complex. It also suggests a common origin for both phases, the molecular phase being gradually dissociated under the combined interaction of the intense radiation field and the strong stellar winds from the nearby massive stars.

Possibly, the Keyhole Nebula was originally part of a larger molecular cloud in which the OB association Tr 16 was shaped. Due to the combined action of the stellar winds and the ionization flux of the young OB cluster, a cavity was blown inside the parental molecular cloud probably nearby the surface. Further interaction caused the molecular surface to break and disperse in the surroundings: the low density gas being photoionized, the denser fragments remaining molecular. In this scenario, the rest of the original cloud corresponds to the molecular cloud which is observed south of Tr 16.

For completeness, we note that an analysis of the energy distribution of η Car from the near-infrared to the decimeter radio range shows that the millimeter emission of this peculiar star is explained by thermal emission from its ionized stellar wind (see also White et al. 1994). A mass-loss rate of $\sim 2.4 \times 10^{-3}$ $M_\odot$ yr^{-1} is derived. Strong flux density variations in the millimeter continuum have also been measured and are likely related to episodic shell ejections leading to variations in the degree of ionization in the wind of η Car (Cox et al. 1995).

4. SUMMARY

The global properties of the Carina Nebula which have been described in this review, based on new radio, infrared and CO line emission studies, are those of a Giant Molecular Cloud such as summarized in Blitz (1993). The Carina Nebula contains two remarkable examples of photon-dominated regions (PDRs) illuminated by the intense ultraviolet radiation from the massive stars of Tr 14 for the northern molecular cloud and the open cluster Tr 16 for the southern cloud. Both PDRs have the additional interest of displaying unusual velocity dispersions which results from the impact of energetic stellar winds (emitted by the most massive members of the clusters) on the molecular cloud surfaces.

An important issue is the apparent paucity of embedded infrared sources. This stays in sharp contrast with other Giant Molecular Clouds such as the Rosette Nebula (Cox, Deharveng, & Leene 1990). Clearly further studies should be done to search for additional embedded infrared sources similar to IRAS 10430–5931 in order to better understand the star formation processes in this outstanding region (see Tapia 1995). The lack of *IRAS* sources could be due to the fact the Carina Nebula is still relatively young. It could also be related to the destructive processes associated with the formation of very massive stars which have inhibited the birth of a next generation of luminous stars through disruption of the parental molecular cloud by stellar winds and dissociating effects from the H II region.

The morphological differences between the PDRs associated with Tr 16 and Tr 14 could reflect age differences, Tr 16 being more evolved than Tr 14. This is consistent with studies of the stellar contents of both clusters (Walborn 1995). However, this difference in evolution does not necessarily imply that star formation proceeded sequentially (Elmegreen & Lada 1977) in the Carina Nebula from south to north as suggested by de Graauw et al. (1981). It is more likely that it occured quasy randomly as suggested by Blitz (1993) to occur in most Giant Molecular Clouds. Triggered star formation can happen locally such as in the case of the embedded source IRAS 10430–5931.

Finally, the processes by which the interstellar medium in the Carina region was assembled into the large cloud complexes which ultimately gave birth to one of the highest concentrations of massive stars known in our Galaxy have still to be identified. Their particular location in the Carina spiral arm may have played a major role through the influence of a density wave shock but further studies are clearly required to settle this question.

J. Whiteoak is kindly thanked for sending his radio data prior to publication. This review greatly benefited from the work done in collaboration with P.J. Roelfsema and T.S. Megeath. L. Bronfman is acknowledged for his constant support during this common project which is part of a CNRS-CONICYT exchange program. Finally, it is a pleasure to warmly thank the organizers of this meeting.

REFERENCES

Bertoldi, F. 1989, ApJ, 346, 735
Blitz, L. 1993, in Protostars and Planets III, ed. E.H. Levy & J.I. Lunine (Tucson: Univ. of Arizona Press), p. 125
Bontekoe, Tj. R., Koper, E., & Kester, D.J.M. 1994, A&A, 284, 1037
Cox, P., Deharveng, L., & Leene, A. 1990, A&A, 230, 694
Cox, P., & Bronfman, L. 1995, ApJ, submitted
Cox, P., Bronfman, L., & Roelfsema, P.J. 1995, in preparation
Cox, P., Mezger, P.G., Sievers, A., Najarro, F., Bronfman, L., Kreysa, E., & Haslam, G. 1995, A&A, submitted
Deharveng, L., & Maucherat, M. 1975, A&A, 41, 27
Dickel, H.R., & Wall, J.V. 1974, A&A, 32, 5
Elmegreen, B.G., & Lada, C.J. 1977, 214, 725
Feinstein, A., Fitzgerald, M.P, & Moffat, A.F.J. 1980, AJ, 85, 708
Feinstein, A. 1995, RevMexAASC, 2, 57
Gardner, F.F., Milne, D.K., Mezger, P.G., & Wilson, T.L. 1970, A&A, 7, 349
Gardner, F.F., Dicke, H.R., & Whiteoak, J.B. 1973, A&A, 23, 51
de Graauw, T., Lidholm, S., Fitton, B., Beckman, J., Israel, F.P., Nieuwenhuijzen, H., & Vermue, J. 1981, A&A, 102, 257
Grabelsky, D.A., Cohen, R.S., Bronfman, L., & Thaddeus, P. 1988, ApJ, 331, 181
Ghosh, S.K., Iyengar,K.V.K., Rengarajan,T.N., Tandon,S.N., Verma,R.P., & Daniel, R.R. 1988, ApJ, 330, 928
Harvey, P.M., Hoffman, W.F., & Campbell, M.F. 1978, A&A, 70, 165
Huchtmeier, W.K., & Day, G.A. 1975, A&A, 41, 153
Malin, D. 1993, A View of the Universe (Cambridge: Cambridge Univ. Press)
Megeath, T.S., Cox, P., Bronfman, L., & Roelfsema, P.J. 1995, in preparation
Retallack, D.S. 1983, MNRAS, 204, 669
Tapia, M. 1995, RevMexAASC, 2, 87
Tateyama, C.E., Strauss, F.M., & Kaufmann, P. 1991, MNRAS, 249, 716
Walborn, N.R. 1975, ApJ, 202, L129
_____. 1991, in IAU Symp. No. 148, The Magellanic Clouds, ed. R. Haynes & D. Milne (Dordrecht: Kluwer), p. 415
_____. 1995, RevMexAASC, 2, 51
Walborn, N.R., Blanco, B.M., & Tackeray, A.D. 1984, ApJ, 219, 498
White, S.M., Duncan, R.A., Lim, J., Nelson, G.J., Drake, S.A., & Kundu, M.R. 1994, ApJ, 429, 380
Whiteoak, J.B., & Otrupcek, R.E. 1984, Proc. ASA, 5, 552
Whiteoak, J.B.Z. 1994, ApJ, 429, 225